

## Effect of Reaction and Regeneration on the Production of Pyridine Bases through Glycerol and Ammonia Route

Cai-Wu Luo<sup>1,\*</sup>, Yong Zhao<sup>1</sup>, Fu-Liang Jiang<sup>1</sup>, Bo Lei<sup>1</sup>,  
Zi-Sheng Chao<sup>2,\*</sup>, Xiang-Yang Li<sup>1,\*</sup>

1. School of Environmental Protection and Safety Engineering, University of South China, Hunan, Hengyang, 421001, China;

2. College of Material Science and Engineering, Changsha University of Science & Technology, Hunan, Changsha, 410114, China

E-mails: [luocaiwu00@126.com](mailto:luocaiwu00@126.com); [450539749@qq.com](mailto:450539749@qq.com).

**Abstract:** The HZSM-22-At-acid and HZSM-5-At-acid catalysts were synthesized by alkaline-acid sequential treatment and the ZnO/HZSM-5-At-acid catalyst was synthesized by wet-impregnated method. Influence factors, including the types of reactors, impurities in glycerol and regeneration, were systematically investigated. The catalysts were characterized by XRD, TG, N<sub>2</sub>-physorption and NH<sub>3</sub>-TPD techniques. The catalytic evaluation showed that the total yield of pyridine bases in the series-connected two-stage reactors was significantly higher than that of the single reactor while the catalytic pair (HZSM-22-At-acid + ZnO/HZSM-5-At-acid) was employed in these reactors, respectively. It was found that the presence of methanol and sodium chloride in glycerol played a great negative effect on the total yield of pyridine bases. The coke was a key factor leading to the deactivation of catalyst. The catalytic activity was basically restored after the regeneration. The total yield of pyridine bases was increased up to 72% after the 6 th reaction, which was obviously higher than that of the similar reports. The characterization results demonstrated that the larger pore size and the declined concentration of acid site (particularly strong acid site) were main reasons for improving the catalytic activity.

**Key words:** Zeolite; Pyridine; Alkaline-treatment; Glycerol; Regeneration.

### 1. Introduction

Pyridine bases including pyridine and its alkyl derivatives (e.g., 2-, 3-, and 4-picolines) have found versatile applications in pharmaceuticals, medicine and pesticides<sup>[1]</sup>, particularly pyridine and 3-picoline. In the early stage, pyridine bases are produced from coal tar extraction, however this pathway suffers from many disadvantages, e.g., complex process, low production and seriously environmental pollution. Nowadays, chemical process using formaldehyde/acetaldehyde/ammonia is mainly constituted the industrial route for the production of pyridine bases<sup>[2]</sup>, but the aldehydes are strong toxicity and prone to polymerization. Moreover, they are from oil resources. Biomass possesses many advantages, e.g., cheap, safety and renewable. The application in the synthesis of high value-added chemicals is of a great interest in the past decades<sup>[3]</sup>. Glycerol is a typical biomass, which is large-scale production as main byproduct during biodiesel process. In recent years, it has been reported that the glycerol/ammonia route is applied for the synthesis of pyridine bases<sup>[4-7]</sup>. For examples, Zhang et al.<sup>[4]</sup> reported that the total yield of pyridine bases over Cu/ZSM-5 was about 43% in a fixed-bed reactor. Our researchers<sup>[7]</sup> studied that the HZSM-5-At (or HZSM-22-At-acid) and ZnO/HZSM-5-At-acid catalysts were respectively added into the first and second stage of reactor, and a higher total yield of pyridine bases was obtained. Obviously, it is a great potential for this route to achieve the industrial manufacture.

The literature<sup>[8]</sup> demonstrated that two different catalysts were filled with the upper and down of the single reactor. However, this mode is no employed in the production of pyridine bases up to date. The crude glycerol from different plants often contains many impurities like methanol and sodium chloride<sup>[9, 10]</sup>. If the impure glycerol is directly applied for the synthesis of pyridine bases, it will significantly reduce the cost of manufacture. Accordingly, it is much meaningful to study them. Besides, a noticeable phenomenon is serious deactivation for the catalysts during the reaction. The researchers agree that the coke is an important factor causing this behavior. It can be mostly burned under air and high temperature, and thus the catalytic activity is basically recovered. Whether to enhance the catalytic activity after many reaction-regeneration cycles is still controversial<sup>[1, 4, 11]</sup>. For examples, Shimizu et al.<sup>[1]</sup> showed that the catalytic activity was difficult to recover due to the presence of the residual carbon accumulation. Zhang et al.<sup>[4]</sup>

considered that the dealumination of catalyst and the part loss of Cu species resulted in the declined catalytic activity. Recently, our groups [11] reported that alkaline-acid sequential treatment ZSM-5-based catalyst was used for the synthesis of pyridine bases from the reaction of acrolein diethyl acetal and ammonia. The results showed that the catalytic activity was significantly increased after many reaction-regeneration cycles. However, this phenomenon is no report in the production of pyridine bases through glycerol and ammonia pathway so far.

In this paper, based on our previous literature [7], the catalyst pair (HZSM-22-At-acid + ZnO/HZSM-5-At-acid) is selected due to its strong catalytic performance. Several factors like impurities in glycerol and regeneration are investigated in detail. A ca. 72% total yield of pyridine bases can be afforded by regenerating HZSM-22-At-acid as the first catalyst and ZnO/HZSM-5-At-acid as the second catalyst in two-stage reactor mode, which is the highest in the glycerol/ammonia route.

## 2. Experimental

### 2.1. Chemicals

All the chemicals, such as glycerol, ammonia, sodium hydroxide, hydrochloric acid, and ammonium chloride, were commercially available and had analytic purity. HZSM-5 (Si/Al = 25) and HZSM-22 (Si/Al = 69) were supplied by Nankai University and Jiangsu Aoke Company, respectively, and they were calcined at 550 °C for 4 h before use.

### 2.2. Catalyst Preparation

The methods of HZSM-22-At-acid and ZnO/HZSM-5-At-acid catalysts are the same as the literature [7]. All the above-described catalysts were first pressed into disks and then crushed and sieved to 20-40 mesh before use.

### 2.3. Catalyst Characterization

X-ray diffraction (XRD) spectroscopy was performed with a Bruker D8-Advance X-ray diffraction instrument. N<sub>2</sub>-physisorption was conducted on a Quantachrome Autosorb-1 instrument at liquid-N<sub>2</sub> temperature. Before measurement, the specimen was in situ outgassed in the instrument at 300 °C for 12 h under a vacuum of 10<sup>-8</sup> Torr. The pore size distribution was determined by the Barrett-Joyner-Halenda (BJH) model. Ammonia temperature-programmed desorption (NH<sub>3</sub>-TPD) profile was recorded by a Micromeritics AutoChem II 2920 analyzer equipped with a TCD detector.

Thermogravimetry (TG) profiles were recorded on a Diamond instrument (Perkin Elmer Corp.).

### 2.4. Catalytic Performance Evaluation

The reaction process is the same as that of the literature [7]. The regenerated catalyst is obtained after the fifth regeneration.

## 3. Results and Discussion

### 3.1 Effect of types of reactors

Figure 1 shows the effect of different reactors over the catalyst pair (HZSM-22-At-acid+ZnO/HZSM-5-At-acid) on the total yield of pyridine bases. One can see that the total yield of pyridine bases is only ca. 14 % while the catalyst pair is respectively added into the upper and down of the single reactor. For comparison, the total yield of pyridine bases is as high as ca. 61 % while they are respectively filled in the first and second stage of reactor in series-connected two-stage reactors. Obviously, using the same the catalyst pair, the yield of the targeted product is large difference in the different reactors. The pathway is that acrolein as the most important product is initially formed from the dehydration of glycerol over the acid catalyst and other products like acetol and acetaldehyde are also produced. Then, these dehydration products react with ammonia to finally form several pyridine bases, e.g., pyridine, 2-picoline and 3-picoline. Generally, the optimal temperatures in the dehydration of glycerol to acrolein are 280 ~ 350 °C while the similar temperature regions in the condensation of acrolein and ammonia were located at 400 ~ 450 °C. It has been reported that HZSM-22-At-acid showed excellent catalytic activity in the dehydration of glycerol to acrolein at 400 °C [12]. Although this temperature is closed to the optimal temperature in the formation of pyridine bases, the total yield of pyridine bases is still extremely low. In this case, reaction temperature is not a key factor for the formation of pyridine bases. To some extent, it indicates that a suitable reactor is very important in this reaction. The literature [13] demonstrated that Brønsted acid sites on the catalyst were in favor of generating acrolein, whereas acetol was easily obtained on the Lewis acid sites of catalyst. Acrolein reacts with ammonia to produce pyridine bases with higher yield, as compared to acetol [4]. In this study, some glycerol over HZSM-22-At-acid is dehydrated into acrolein while others glycerol is entered

into the ZnO/HZSM-5-At-acid catalyst. Because ZnO/HZSM-5-At-acid contains Brønsted acid sites and Lewis acid sites [7]. In this case, it plays a great negative effect on the catalytic properties. In addition, ammonia can poison the acid sites of catalyst. Therefore, the yields of pyridine bases are very low. Using series-connected two-stage reactor, these adverse influences are eliminated as much as possible and thus the total yield of pyridine bases is dramatically increased.

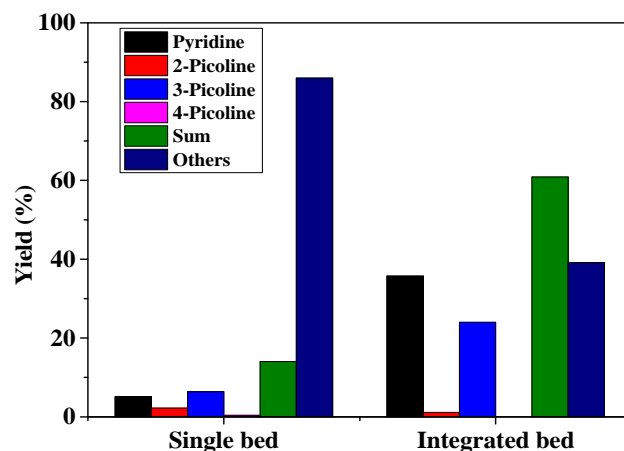


Fig. 1 Effect of different reactors.

(1) a single bed: HZSM-22-At-acid (upper) + ZnO/HZSM-5-At-acid (down), reaction temperature = 425 °C, LHSV = 0.60 h<sup>-1</sup>, concentration of glycerol = 36 wt%, glycerol/ammonia = 1/4, TOS = 1 ~ 3 h.

(2) an integrated bed: HZSM-22-At-acid is filled in the first stage of reactor, reaction temperature = 400 °C, ZnO/HZSM-5-At-acid is filled in the second stage of reactor, reaction temperature = 425 °C, LHSV = 0.45 h<sup>-1</sup>, concentration of glycerol = 20 wt%, glycerol/ammonia = 1/5, TOS = 1 ~ 3 h. Sum = pyridine + 2-picoline + 3-picoline + 4-picoline. Others are denoted as reaction byproducts.

### 3.2 Effect of impurities in glycerol

Figure 2 displays the effect of impurities in glycerol on the total yield of pyridine bases. One can see that the total yield of pyridine bases is as high as ca. 61% while employing pure glycerol as start material. For comparison, the total yield of pyridine bases is only ca. 31% using the impure glycerol. It shows that the impurities in glycerol have an obviously negative impact on the total yield of pyridine bases. It is good agreement with the literature [14]. On the one hand, methanol may compete with glycerol on the catalytic sites and therefore it reduces the dehydration of glycerol to acrolein. Meanwhile, it may react with acrolein to acetal [15, 16]. On the other hand, NaCl as a salt covers and/or neutralizes the acid sites of HZSM-22-At-acid and/or ZnO/HZSM-5-At-acid catalysts. In this case, the catalytic sites are significantly decreased. Moreover, Na ion can accelerate the polymerization of acrolein. Accordingly, these factors result in decreasing the total yield of pyridine bases.

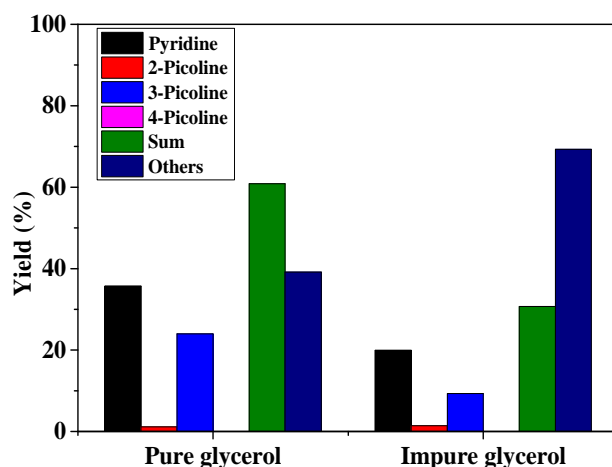


Fig. 2 Effect of impurities in glycerol.

Reaction conditions: HZSM-22-At-acid is filled in the first stage of reactor, reaction temperature = 400 °C, ZnO/HZSM-5-At-acid is filled in the second stage of reactor, reaction temperature = 425 °C, LHSV = 0.45 h<sup>-1</sup>,

concentration of glycerol = 20 wt%, glycerol/ammonia = 1/5, TOS = 1 ~ 3 h. Methanol = 10 wt%, NaCl = 10 wt%. Content of impurities = (methanol or NaCl) / (glycerol + methanol + NaCl). Sum = pyridine + 2-picoline + 3-picoline + 4-picoline. Others are denoted as reaction byproducts.

### 3.3 Effect of regeneration

Figure 6 displays the effect of regeneration on the total yield of pyridine bases. One can see that the color becomes from white to black in the used catalyst, as compared to the fresh catalyst, implying that the coke is main reason leading to the deactivation of catalyst. After the regeneration, the total yield of pyridine bases still as high as 60%. It demonstrates that the regenerated catalyst basically retains the initial catalytic activity. Simultaneously, the coke is effectively removed by using the regeneration in this work. The total yield of pyridine bases is increased up to ca. 72% while the sixth reaction is operated. The fact shows that the catalytic activity is enhanced after running several reaction-regeneration cycles. This is consistent with the literature<sup>[11]</sup>.

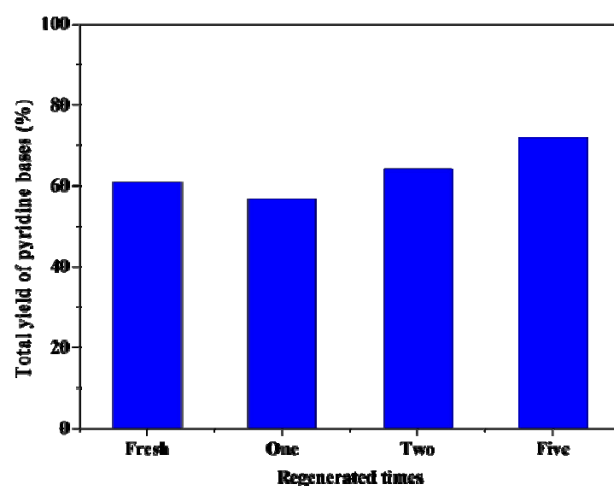


Fig. 3 Effect of the regeneration.

Reaction conditions: HZSM-22-At-acid is filled in the first stage of reactor, reaction temperature = 400 °C, ZnO/HZSM-5-At-acid is filled in the second stage of reactor, reaction temperature = 425 °C, LHSV = 0.45 h<sup>-1</sup>, concentration of glycerol = 20 wt%, glycerol/ammonia = 1/5. Regeneration conditions: reaction temperature = 450 ~500 °C, air and water.

Table 1 compares the results about the reaction of glycerol and ammonia toward pyridine bases. In a single reactor, employing Cu/HZSM-5<sup>[4]</sup>, HZSM-5<sup>[5]</sup> and nano-sized HZSM-5<sup>[6]</sup>, the total yield of pyridine bases are respectively 43%, 36% and 42%. In a series-connected two-stage reactor<sup>[7]</sup>, as high as ca. 62% and 61% total yield of pyridine bases are obtained over the catalyst pairs (HZSM-5-At+ ZnO/HZSM-5-At-acid) and (HZSM-22-At-acid+ZnO/HZSM-5-At-acid), respectively. In this work, the total yield of pyridine bases is up to ca. 72%, while using regenerated the catalyst pair (HZSM-22-At-acid + ZnO/HZSM-5-At-acid). This value is the highest among the reported literature in the glycerol/ammonia route.

Table 1 Comparison with the results *via* glycerol and ammonia route

Reactor Mode	Catalysts	Pyridine bases <sup>a</sup> (%)	Ref.
Single reactor	Cu/HZSM-5	43	[4]
	HZSM-5	36	[5]
	nano-sized HZSM-5	42	[6]
Two-stage reactor	HZSM-5-At + ZnO/HZSM-5-At-acid	62	[7]
	HZSM-22-At-acid + ZnO/HZSM-5-At-acid	61	
	Regenerated (HZSM-22-At-acid+ ZnO/HZSM-5-At-acid)	72	This work

<sup>a</sup> Pyridine bases = pyridine + 2-picoline + 3-picoline +4-picoline.

### 3.4 Characterization

Figure 4 shows the XRD patterns of fresh and regenerated ZnO/HZSM-5-At-acid catalysts. One can see that they both exhibit the characteristic peaks of ZSM-5 zeolite, without the diffraction peaks for other phases. It indicates that the structure of ZSM-5 zeolite is retained after running a long time. Moreover, no ZnO phase ( $2\theta = 31.1^\circ, 34.1^\circ, 36.1^\circ$  and  $56.2^\circ$ ) has been identified by XRD, showing that ZnO has a very small dimension, either being unable to be detected by XRD or highly dispersed on ZSM-5 zeolite.

Figure 5 displays the TG-DSC profiles of the used HZSM-22-At-acid and ZnO/HZSM-5-At-acid catalysts. One can see that the mass loss is small at below  $425^\circ\text{C}$  in the both used catalyst, which is attributed to the adsorbed water and the low-boiling products. For the used HZSM-22-At-acid catalyst, a large and small mass loss are occurred at  $400 \sim 600^\circ\text{C}$  and  $600 \sim 900^\circ\text{C}$ , respectively. It shows that two types of the coke are appeared on the basis of the DSC profile. For the used ZnO/HZSM-5-At-acid catalyst, a larger mass loss appeared at  $400 \sim 700^\circ\text{C}$ . In other words, the coke isn't completely removed under regeneration condition in this work. Therefore, it is reasonably concluded that the regenerated ZnO/HZSM-5-At-acid catalyst contains indeed a little coke.

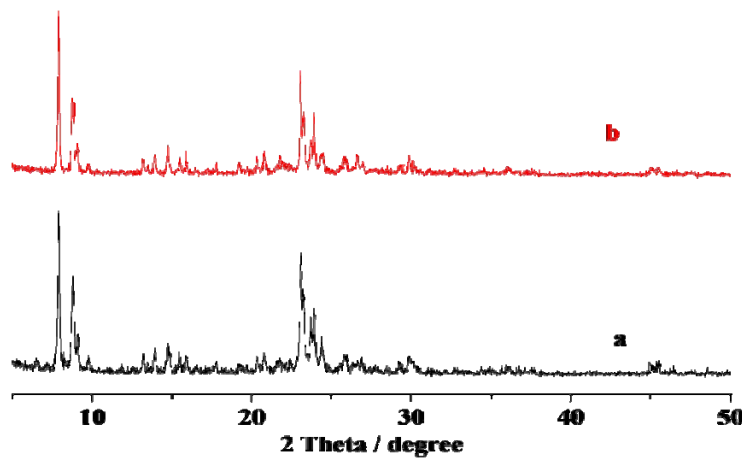


Fig. 4 XRD patterns of various catalysts: fresh (a) and regenerated (b) ZnO/HZSM-5-At-acid catalysts.

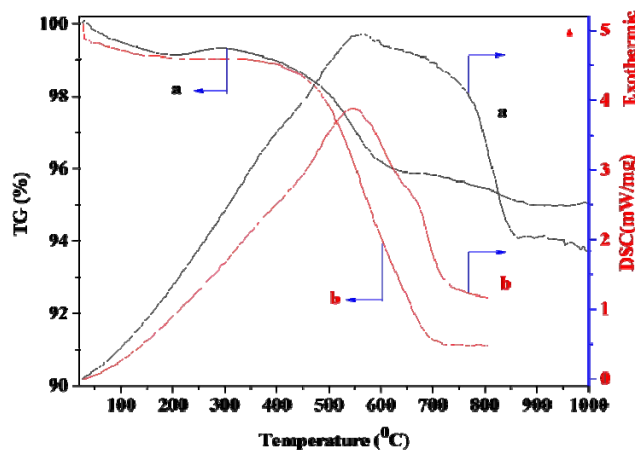


Fig. 5 TG-DSC profiles of used HZSM-22-At-acid (a) and ZnO/HZSM-5-At-acid (b) catalysts.

Figure 6 (left) displays the  $\text{N}_2$  adsorption-desorption isotherms for fresh and regenerated ZnO/HZSM-5-At-acid catalysts and the corresponding pore size distribution profiles for the catalysts are shown in Figure 6 (right). One can see from Figure 6 (left) that the isotherms for the both catalysts rise rapidly at  $P/P_0 < 0.1$ , which belong to I type, being characteristic of microporous zeolites. The both above isotherms contain a hysteresis loop of H4 type, which is indicative of the presence of mesopores with irregular and

slitlike shape in the catalysts. Furthermore, the hysteresis loop becomes larger in the regenerated ZnO/HZSM-5-At-acid catalyst, relative to the fresh ZnO/HZSM-5-At-acid one, implying that more mesopores are generated. The mesopores may be most probably generated as the intercrystal voids *via* the aggregation of zeolites crystals and/or as the intracrystal cavities *via* the dealumination by the reaction-regeneration treatment. From Figure 6 (right), one can see that the pore sizes for the fresh and regenerated ZnO/HZSM-5-At-acid catalysts are both distributed at 3.8 nm. Besides, an additional micropore size is newly appeared at 1.7 nm. The addition micropores may be generated within the zeolite crystals *via* dealumination of the regenerated ZnO/HZSM-5-At-acid catalyst during reaction and/or regeneration.

Table 2 displays the textual properties determined from N<sub>2</sub> adsorption - desorption experiments for fresh and regenerated ZnO/HZSM-5-At-acid catalysts. One can see that, from fresh ZnO/HZSM-5-At-acid to regenerated ZnO/HZSM-5-At-acid catalysts, the BET specific surface area ( $S_{BET}$ ), micropore surface area ( $S_{micro}$ ), and external surface area ( $S_{ext}$ ) are all decreased. This is due to the fact that the partial dealumination happens during the reaction and/or regeneration, thereby, leading to generating the larger micropore size. Meanwhile, a proportion of the extracted Al species can be re-deposited to block partially the channels of ZSM-5 zeolite, resulting in the decrease in the surface area. Besides, the residual coke covers and/or blocks the pore structure, even after the regeneration.

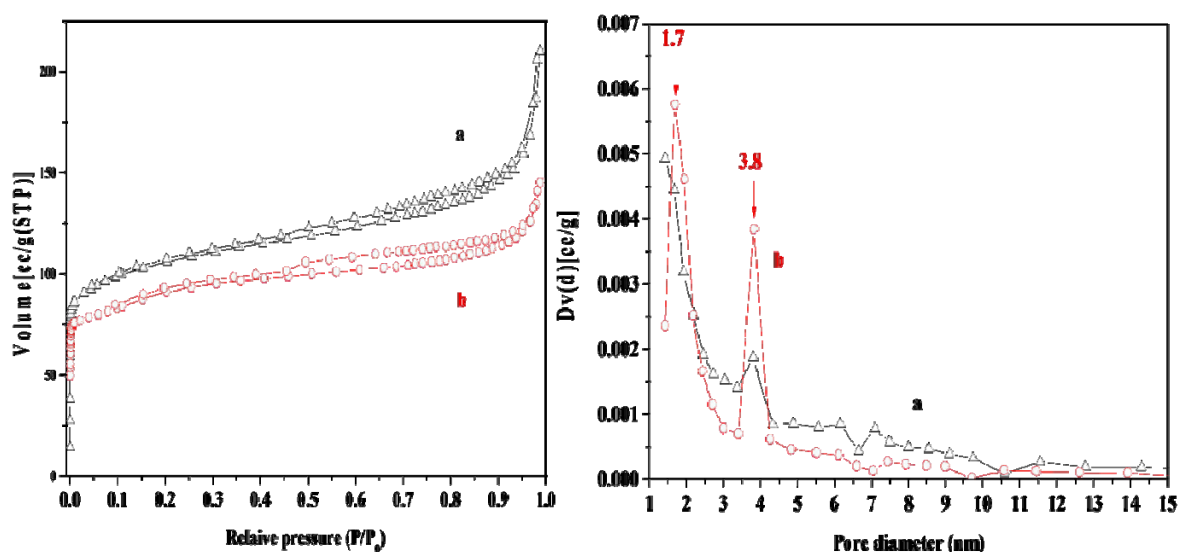


Fig. 6 N<sub>2</sub> adsorption-desorption isotherms (left) and pore size distributions (right) of fresh (a) and regenerated (b) ZnO/HZSM-5-At-acid catalysts.

Table 2 Results of BET over fresh and regenerated ZnO/HZSM-5-At-acid catalysts

Samples	$S_{BET}$ (m <sup>2</sup> /g)	$S_{micro}$ (m <sup>2</sup> /g)	$S_{ext}$ (m <sup>2</sup> /g)
Fresh	372.1	284.6	87.5
Regenerated	329.4	271.5	57.9

Table 3 Results of acidity over fresh and regenerated ZnO/HZSM-5-At-acid catalysts

Samples	$T_{m,1}$ (< 300 °C)	$T_{m,2}$ (> 300 °C)	$A_{total}$ (mmol/g)
	$A_1$ (mmol/g)	$A_2$ (mmol/g)	
Fresh	0.62	0.58	1.20
Regenerated	0.38	<i>N. V</i>	0.38

Figure 7 displays the NH<sub>3</sub>-TPD profiles of the fresh and regenerated ZnO/HZSM-5-At-acid catalysts, and the temperature at the maximum ( $T_{m,i}$ ) and integral area ( $A_i$ ) of desorption peak, referring to the strength and concentration of acid site, respectively, are listed in Table 3. For the fresh ZnO/HZSM-5-At-acid catalyst, two distinct desorption peak centering at below 300 °C ( $T_{m,1}$ ) and at above 300 °C ( $T_{m,2}$ ), respectively. The  $T_{m,1}$  and  $T_{m,2}$  peaks over the fresh ZnO/HZSM-5-At-acid catalyst can be attributed to the weak acid site caused by the silanol group, and the strong acid site associated with bridge hydroxyl group (Brønsted acid site) and the species from the interaction between ZnO and HZSM-5 zeolite. For the

regenerated ZnO/HZSM-5-At-acid catalyst, only one desorption peak is found at below 300 °C. It shows that the strong acid site in the regenerated ZnO/HZSM-5-At-acid catalyst is completely disappeared. This is the most probably that the dealumination from the framework of ZSM-5 zeolite is occurred and thus it leads to reducing the strong acid site. Additionally, the residual carbon deposition covers the acid sites of catalyst, leading to decreasing the concentrations of weak acid site and strong acid site. Accordingly, the total concentration of acid site in the regenerated ZnO/HZSM-5-At-acid catalyst is significantly decreased, as compared to the fresh ZnO/HZSM-5-At-acid one. Combined with the catalytic results, it can be concluded that the weak acid site is responsible for catalyzing the formation of pyridine bases.

In a word, the partial dealumination and the residual coke in the regenerated ZnO/HZSM-5-At-acid catalyst are happened after several reaction-regeneration cycles, thereby, resulting in strengthening the catalytic activity. The reasons are as follows: (1) the dealumination can enlarge the pore size and lower the concentration of acid sites. The large pore size is in favor of speeding up the mass transfer rate; the polymerization of intermediates like acrolein is slowed down because of the reduced concentration of acid site, particularly strong acid site; (2) the residual coke can enhance the hydrophobicity of catalyst and also reduce the total concentration of acid site. This hydrophobicity can to some extent prevent water from covering the catalytic site. Besides, the coke is preferentially deposited on the strong acid site and thus the side reactions are decreased. Therefore, a larger total yield of pyridine bases can be achieved over the regenerated catalyst after several reaction-regeneration cycles.

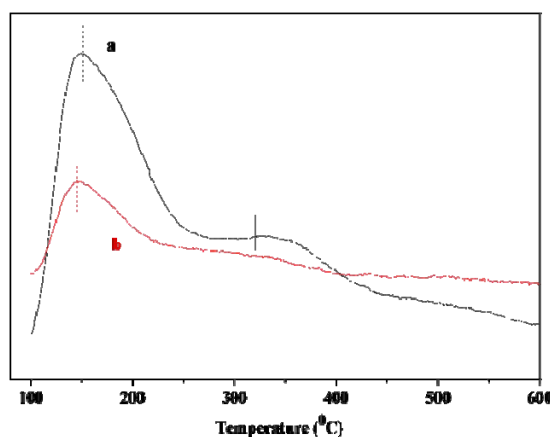


Fig.7 NH<sub>3</sub>-TPD profiles of fresh (a) and regenerated (b) ZnO/HZSM-5-At-acid catalysts.

#### 4. Conclusion

- 1) The total yield of pyridine bases was significantly increased while HZSM-22-At-acid and ZnO/HZSM-5-At-acid were respectively employed in the first reactor and the second reactor in two-stage reactor mode, relative to them locating the upper and down of a single reactor;
- 2) The impurities in glycerol had a great negative effect on the total yield of pyridine bases, arising from accelerating the polymerization of acrolein and reducing the acid sites of catalyst;
- 3) The coke was main reason for the deactivation of catalyst in this reaction. By regeneration, the coke was effectively removed and therefore the catalytic activity was basically recovered. After several reaction-regeneration cycles, the total yield of pyridine bases reached ca. 72%. The value was the highest in the glycerol/ammonia route. The characterization revealed that the pore size was enlarged and the amount of acid sites was significantly reduced. These factors resulted in enhancing the catalytic activity.

#### 5. References

- [1] Shimizu S, Abe N, Iguchi A, et al. Synthesis of pyridine base: General methods and recent advances in gas phase synthesis over ZSM-5 zeolite [J]. Catal. Surv. Jpn. 1998, 2 (1): 71-78.
- [2] Reddy K R S K, Sreedhar I, Raghavan K V. Interrelationship of process parameters in vapor phase pyridine synthesis [J]. Appl. Catal. A: General. 2008, 339 (1): 15-20.
- [3] Mirkouei A, Haapala K R, Sessions J, et al. A review and future directions in techno-economic modeling and optimization of upstream forest biomass to bio-oil supply chains [J]. Renew. Sust. Energ. Rev. 2017, 67: 15-35.
- [4] Zhang Y C, Yan X, Niu B Q, et al. A study on the conversion of glycerol to pyridine bases over

Cu/HZSM-5 catalysts [J]. *Green Chem.* 2016, 18: 3139-3151.

[5] Xu L J, Han Z, Yao Q, et al. Towards the sustainable production of pyridines via thermo-catalytic conversion of glycerol with ammonia over zeolite catalysts [J]. *Green Chem.* 2015, 17: 2426-2435.

[6] Xu L J, Yao Q, Zhang Y, et al. Producing pyridines via thermo-catalytic conversion and ammonization of glycerol over nano-sized HZSM-5 [J]. *RSC Adv.* 2016, 6: 86034-86042.

[7] Luo C W, Huang C, Li A, et al. Influence of reaction parameters on the catalytic performance of alkaline-treated zeolites in the novel synthesis of pyridine bases from glycerol and ammonia [J]. *Ind. Eng. Chem. Res.* 2016, 55 (4): 893-911.

[8] Witsuthammakul A, Sooknoiil T. Direct conversion of glycerol to acrylic acid via integrated dehydration-oxidation bed system [J]. *Appl. Catal. A: General.* 2012, 413-414: 109-116.

[9] Kong P S, Aroua M K, Daud W M A W. Conversion of crude and pure glycerol into derivatives: A feasibility evaluation [J]. *Renew. Sust. Energ. Rev.* 2016, 63: 533-555.

[10] Seretis A, Tsiakaras P. Crude bio-glycerol aqueous phase reforming and hydrogenolysis over commercial SiO<sub>2</sub> single bond Al<sub>2</sub>O<sub>3</sub> nickel catalyst [J]. *Renew. Energ.* 2016, 97: 373-379.

[11] Luo C W, Feng X Y, Liu W, et al. Deactivation and regeneration on the ZSM-5-based catalyst for the synthesis of pyridine and 3-picoline [J]. *Microporous Mesoporous Mater.* 2016, 235: 261-269.

[12] Hoang T Q, Zhu X L, Danuthai T, et al. Conversion of glycerol to alkyl-aromatics over zeolites [J]. *Energ. Fuel.* 2010, 24: 3804-3809.

[13] Alhanash A, Kozhevnikova E F, Kozhevnikov I V. Gas-phase dehydration of glycerol to acrolein catalysed by caesium heteropoly salt [J]. *Appl. Catal. A: General.* 2010, 378 (1): 11-18.

[14] Luo C W, Feng X Y, Chao Z S. Microwave-accelerated direct synthesis of 3-picoline from glycerol through a liquid phase reaction pathway [J]. *New J. Chem.* 2016, 40: 8863-8871.

[15] Luo C W, Li A, An J F, et al. The synthesis of pyridine and 3-picoline from gas-phase acrolein diethyl acetal with ammonia over ZnO/HZSM-5 [J]. *Chem. Eng. J.* 2015, 273: 7-18.

[16] Luo C W, Chao Z S. Unsaturated aldehydes: a novel route for the synthesis of pyridine and 3-picoline [J]. *RSC Adv.* 2015, 5: 54090-54101.